# Utilization of Plant Ash for the Fabrication of Novel Superabsorbent Composites with Potassium-Release Characteristics

**Wenbo Wang,[1,2] Aiqin Wang[1]**

[1]*Center for Eco-material and Green Chemistry, Lanzhou Institute of Chemical Physics, Chinese Academy of Sciences, Lanzhou 730000, People's Republic of China*
[2]*Graduate University of the Chinese Academy of Sciences, Beijing 100049, People's Republic of China*

Received 15 April 2009; accepted 15 August 2009
DOI 10.1002/app.31306
Published online 7 October 2009 in Wiley InterScience (www.interscience.wiley.com).

**ABSTRACT:** Design and synthesis of the agricultural and ecological superabsorbent materials with cost-efficient and fertilizer-release characteristics has recently attracted considerable interests. In this work, the novel poly(sodium-potassium acrylate-*co*-acrylamide)/plant ash (PNa-KA-*co*-AM/PA) superabsorbent composites with potassium-release characteristics were prepared using partially neutralized acrylic acid (Na-KA), acrylamide (AM), and plant ash (PA) as raw materials, ammonium persulfate (APS) as the initiator, and *N*,*N*′-methylenebisacrylamide (MBA) as the crosslinker. The structure, morphologies, and thermal stability of the composites were characterized by Fourier transform infrared spectrophotometer, scanning electron microscopy, and TGA techniques, respectively. The effects of MBA concentration and PA content on water absorbency were studied, and the swelling properties of the composites in saline solutions and various pHs solution as well as their potassium-release capabilities were also evaluated. Results indicate that the composites exhibit better thermal stability, salt-resistant performance, pH-stability, and potassium-release properties, and can act as a fertilizer and an effective water-saving material for agricultural and ecological application. © 2009 Wiley Periodicals, Inc. J Appl Polym Sci 115: 1814–1822, 2010

**Key words:** superabsorbent composite; plant ash; potassium fertilizer release; swelling; water retention

## INTRODUCTION

As a preponderant water-saving material, superabsorbent has found promising application in modern agriculture due to its unique advantages of absorbing and retaining much water over traditional absorbents.[1–3] In the past decades, the researches on superabsorbent are mainly focused on reducing production cost and enhancing water-absorbing capabilities. Little efforts regarding the development of the superabsorbent with fertilizer-release properties despite it was known that the growth and quality of plants or crops are affected by both water and fertilizers. Previous investigations[4,5] have confirmed that about 40–70% fertilizer was lost to the environment and failed to be absorbed by plants when it was directly mixed with soil; this results in the large resource losses and serious environmental pollution. Presently, the most effective method of reducing fertilizer losses involves the use of slow- or controlled-release fertilizers, and some fertilizer-release superabsorbents have been developed.[6–11] Among them, the direct compounding of organic polymer with other functional filler, such as, sodium humate for deriving multicomponent superabsorbent was considered as a simple and preferred method.[12–15] The incorporation of the available fertilizer in nature can realize the synchronous improvement of water-absorbing and fertilizer-release properties.

Plant ash (PA) is the residue after the herbaceous or woody plant being burnt. PA contains almost all the elements existed in the plant,[16] and it was usually used as a kind of easily available, low-cost, and nutrient-fertile inorganic fertilizer. In the numerous components of PA, the content of potassium that is essential to the growth of plant is higher. By virtue of this, PA has long exhibited great potentials in the design and fabrication of potassium fertilizer as a resource of potassium. Currently, the multifunctional superabsorbents with fertilizer-release properties

*Correspondence to:* A. Wang (aqwang@lzb.ac.cn).
Contract grant sponsor: West Light Foundation and the Western Action Project of CAS; contract grant number: KGCX2-YW-501.
Contract grant sponsor: "863" Project of the Ministry of Science and Technology; contract grant numbers: 2006AA03Z0454, 2006AA100215.

prepared through the compounding of natural fertilizer with organic superabsorbent have attracted great interest. So the novel superabsorbent with improved water-saving property, reduced production cost, and excellent fertilizer-release capability was expected to be produced by introducing PA into superabsorbent network.

On the basis of above background, in this article, the novel poly(sodium-potassium acrylate-*co*-acrylamide)/plant ash (PNa-KA-*co*-AM/PA) superabsorbent composites were prepared through a solution polymerization reaction by using PA as a functional component. The structure and morphology of the developed composite was characterized by Fourier transform infrared (FTIR) spectrophotometer and scanning electron microscopy (SEM). In addition, the swelling behaviors and potassium fertilizer-release properties of the superabsorbent composites were evaluated systematically.

## EXPERIMENTAL

### Materials

Acrylic acid (AA, chemically pure, Shanghai Shanpu Chemical Factory, Shanghai, China) was distilled under reduced pressure before use. Ammonium persulfate (APS, analytical grade, Xi'an Chemical Reagent Factory, China) was used as received. *N*,*N*′-methylenebisacrylamide (MBA, chemically pure, Shanghai Chemical Reagent Corp., China) was used as purchased. PA micropowder (XianTao Chishun Carbon Co., Hubei, China) was milled and passed through a 320-mesh screen (diameter is about 46 μm) before use. All other reagents used were all of analytical grade and all solutions were prepared with distilled water.

### Preparation of PNa-KA-*co*-AM/PA and PNaA-*co*-AM superabsorbents

AA (3.93 g) was dissolved in 18 mL distilled water in a 250-mL four-necked flask equipped with a mechanical stirrer, a reflux condenser, a thermometer, and a nitrogen line. The resultant solution was neutralized using 2.37 mL 8.80 mol/L NaOH to reach a total neutralization degree of 57% (the amount of alkaline PA was calculated as part of neutralization degree, and the equivalent relationship between PA and NaOH solution was defined as follows: 1.00 g PA = 0.6218 mL 8.80 mol/L NaOH solution). Then, crosslinker MBA (14.40 mg), acrylamide (AM) (3.27 g), and PA micropowder (1.84 g) was added to the neutralized AA solution. After the mixture was de-oxygen for 30 min under mechanical stirring, 10 mL aqueous solution of initiator APS (0.1152 g) was charged into the reaction flask and the reactant was slowly heated to 70°C in an oil bath, and maintained for 3 h to finish the polymerization. A nitrogen atmosphere was maintained throughout the reaction period. The final gel products were dried to constant weight in an oven at 70°C; the dried samples were ground and passed through a 40–80 mesh sieve (180–380 μm). PNaA-*co*-AM superabsorbent hydrogel was prepared according to a similar procedure except without PA.

### Measurements of equilibrium water absorbency and swelling kinetics

Sample (about 0.05 g) was immersed in excess aqueous liquids at room temperature for 4 h to reach a swelling equilibrium. The swollen samples were filtered using a 100-mesh screen and then drain on the screen for 10 min to remove the redundant water. After weighing the swollen samples, the equilibrium water absorbency of superabsorbents can be calculated using Eq. (1).

$$Q_{eq} = (w_2 - w_1)/w_1 \quad (1)$$

$Q_{eq}$ is the equilibrium water absorbency calculated as grams of water per gram of the sample; $w_1$ and $w_2$ are the weights of the dry sample and water-swollen sample, respectively.

Swelling kinetics of superabsorbents in distilled water was determined as follows: an accurate amount of samples (0.05 g) were placed in 500 mL beakers, and then 400 mL of distilled water was poured into the beakers. The swollen gels were separated using a 100-mesh sieve at set intervals, and the water absorbency of superabsorbents at a certain moment was determined by weighing the swollen samples and then calculated according to Eq. (1). All samples were carried out thrice repeatedly and the averages are reported in this article.

### Measurement of water absorbency in various pH solutions

The pH values of solution were adjusted by the aqueous solution of HCl (pH = 2) or NaOH (pH = 13). The method of determining water absorbency of superabsorbents in various pH solutions is similar with that in distilled water.

### Measurement of potassium-release properties

The sample (about 0.10 g) was immersed in 400 mL distilled water, and the swollen samples were filtered at set intervals (1, 3, 5, 10, 20 30, 60, 120, and 360 min). The filtrate was collected and transferred into a 500 mL volumetric flask and diluted to the scale plate. The concentration of $K^+$ (mg/L) was

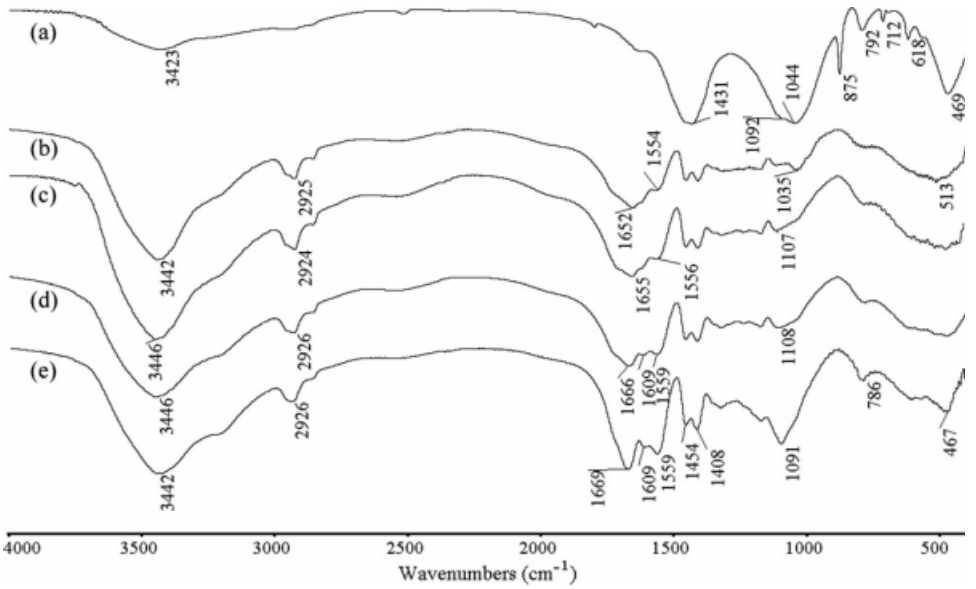


**Figure 1** FTIR spectra of (a) PA, (b) PNaA-*co*-AM, and (c–e) PNa-KA-*co*-AM/PA containing 10, 20, and 30 wt % of PA, respectively.

determined by atomic absorption spectrum analysis, and the potassium-release amounts were expressed using the mass of potassium released from 1 g of sample (mg/g).

### Characterizations

FTIR spectra were recorded on a Nicolet NEXUS FTIR spectrometer in 4000 $cm^{-1}$ to 400 $cm^{-1}$ region using KBr pellets. Thermal stability of samples was studied on a PerkinElmer TGA-7 thermogravimeric analyzer (PerkinElmer Cetus Instruments, Norwalk, CT), with a temperature range of 25–800°C at a heating rate of 10°C/min using dry nitrogen purge at a flow rate of 50 mL/min. The morphologies of the samples were examined using a JSM-5600LV SEM instrument (JEOL) after coating the sample with gold film. The concentration of $K^+$ in the lixivium of the composites was determined by a 180/80 atomic absorption spectrophotometer (Hitachi, Japan).

## RESULTS AND DISCUSSION

### FTIR spectra analysis

The structure of the composite was characterized by FTIR technique and the spectrogram was shown in Figure 1. As can be observed, the bands of PA at 1431 $cm^{-1}$ and 875 $cm^{-1}$ (the characteristic absorption of carbonate existed in PA) disappeared after reaction, which indicates that the carbonate participated reaction. The bands of PA at 1092 (asymmetrical stretching of Si—O—Si), 1044 $cm^{-1}$ (asymmetrical stretching of Si—O), 792 $cm^{-1}$ (symmetrical stretching of Si—O—Si), and 618 $cm^{-1}$ (symmetrical stretching of Si—O) almost disappeared in the spectra of PNa-KA-*co*-AM/PA (10 wt % and 20 wt %), indicating that the $SiO_2$ in PA also takes part in polymerization reaction through its active Si—OH groups.[17] However, these peaks can be observed in the spectrum of PNa-KA-*co*-AM/PA containing 30 wt % PA, this information implied that the excess PA was physically filled in the polymer network. The absorption bands of PNaA-*co*-AM at 1652 $cm^{-1}$, 1604 $cm^{-1}$, 1554 $cm^{-1}$, and 1296 $cm^{-1}$ were assigned to the —C=O of —COOH, the amide I, the overlapping peak of amide II and —C=O of —$COO^-$ groups, and the amide III, respectively. The bands of amide are not obvious in PNaA-*co*-AM due to the strong hydrogen bonding interaction among —COOH, —$COO^-$, and C=O($NH_2$) groups. However, the characteristic bands of amide become evident with the incorporation of PA and the increase of amount of PA. The absorption of —COOH and —$COO^-$ groups shifted to high wave-number region (from 1652 to 1669 $cm^{-1}$ for —COOH and from 1554 to 1559 $cm^{-1}$ for —$COO^-$) and the peak shape becomes more sharp with increasing the content of PA from 10 to 30 wt %, which give a direct evidence that the existence of PA in polymeric network greatly decreased the hydrogen bonding interaction among polymeric chains. By comparison with the FTIR spectra of samples before and after reaction, it can be concluded that PA participates in polymeric reaction and formed a composite.

### Thermal stability

The TGA curves of PNaA-*co*-AM and PNa-KA-*co*-AM/PA with 10, 20, and 30 wt % of PA are depicted

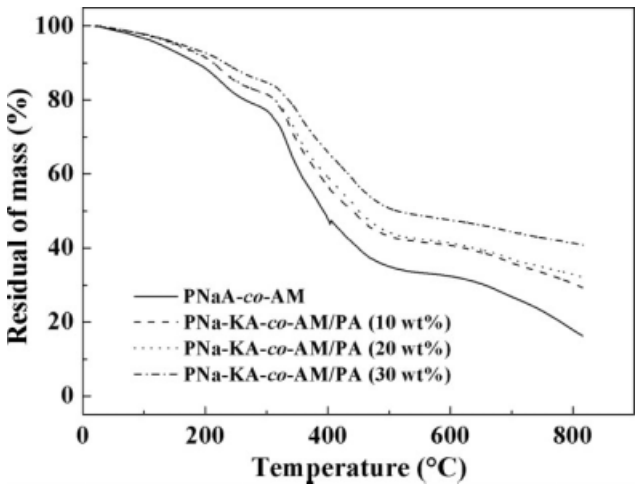


**Figure 2** TGA curves of (a) PNaA-*co*-AM, (b) PNa-KA-*co*-AM/PA (10 wt %), (c) PNa-KA-*co*-AM/PA (20 wt %), and (d) PNa-KA-*co*-AM/PA (30 wt %).

in Figure 2. It can be seen that PNaA-*co*-AM and PNa-KA-*co*-AM/PA composites show a similar weight-loss tendency, but the weight-loss rate of the composites is obviously slower than that of PNaA-*co*-AM. The weight loss about 11.0% below 199.6°C for PNaA-*co*-AM, about 8.2 wt % below 202.9°C for PNa-KA-*co*-AM/PA (10 wt %), about 8.1 wt % below 204.2°C for PNa-KA-*co*-AM/PA (20 wt %), and about 7.9 wt % below 214.5°C for PNa-KA-*co*-AM/PA (30 wt %) was ascribed to the removal of water absorbed and bonded in sample. The minor weight loss about 11.8% (199.6–303.8°C) for PNaA-*co*-AM, and the loss about 10.9 wt % (202.9–314.5°C), about 6.3 wt % (204.2–315.8°C), and about 4.9 wt % (214.5 and 316.5°C) for PNa-KA-*co*-AM/PA with 10, 20, and 30 wt % PA, respectively, can be attributed to the elimination of the water molecule from the two neighboring carboxylic groups of the polymer chains due to the formation of anhydride.[18] The successive weight loss of 45.3 wt % (303.8–625.7°C) for PNaA-*co*-AM, 40.4 wt % (314.5–627.1°C), 39.2 wt % (315.8–637.1°C), and 37.1 wt % (316.5–645.2°C) for PNa-KA-*co*-AM/PA with 10, 20, and 30 wt % PA, respectively, is ascribed to the destruction of carboxylic and amide groups as well as main chain scission. In addition, the residual weight is 29.5 wt % for PNa-KA-*co*-AM/PA (10 wt %), 32.2 wt % for PNa-KA-*co*-AM/PA (20 wt %), and 40.9 wt % for PNa-KA-*co*-AM/PA (30 wt %) but it is only 16.3 wt % for PNaA-*co*-AM at 800°C, indicating that the incorporation of PA can greatly improve the thermal stability of superabsorbent.

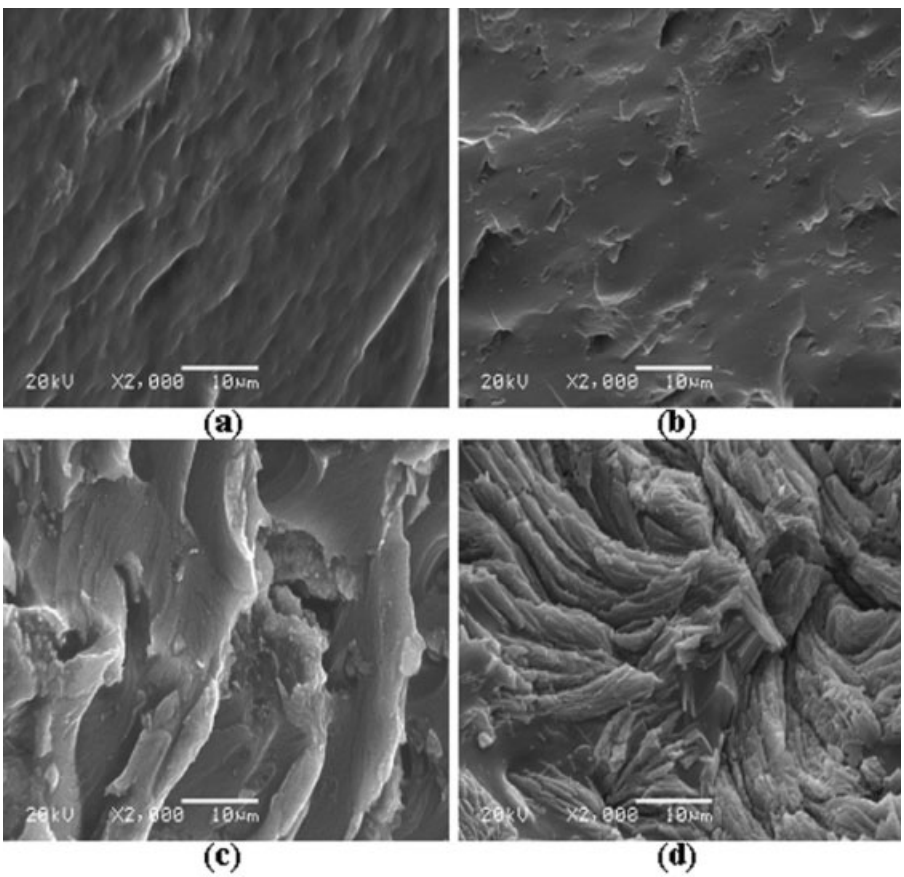


**Figure 3** SEM micrographs of (a) PNaA-*co*-AM and (b–d) PNa-KA-*co*-AM/PA with 10, 20, and 30 wt % of PA, respectively.

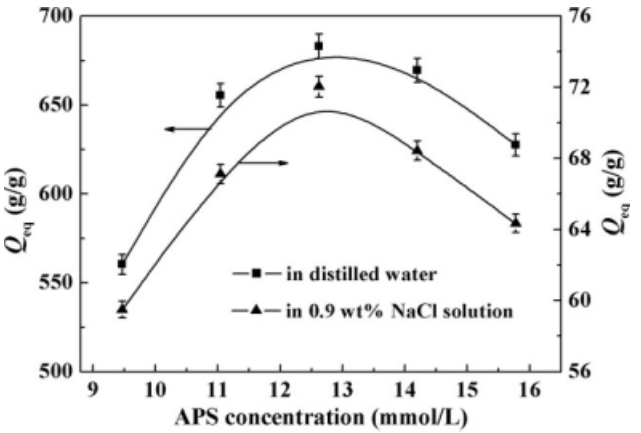


**Figure 4** Effect of APS concentration on water absorbency: molar ratio of AA to AM, 1.2; neutralization degree of AA, 57%; MBA concentration, 2.335 mmol/L; and PA content, 20 wt %.

### Surface morphologies

Figure 3 depicted the SEM micrographs of the superabsorbent composites containing various amounts of PA. It can be seen from Figure 3(a) that PNaA-*co*-AM only exhibit a smooth and dense surface, whereas the superabsorbent composites containing PA show a correspondingly coarse and undulant surface [Fig. 3(b,c)]. The surface roughness of PNa-KA-*co*-AM/PA increased with increasing the content of PA, implying that introduction of PA is favorable to improve the surface structure of the resultant composite. The great morphological changes can be ascribed to the facts that, (i) the silicate in PA participated in the polymerization reaction and the construction of 3D polymer network, and so the hydrophilic network was greatly improved due to the incorporation of rigid silicate and the collapse of superabsorbent network during drying was also prevented; (ii) the carbonate in PA may act as a vesicant, which can decompose and release $CO_2$ gas during reaction, and thus improved the internal and surface structure of the composites.[19] Moreover, it can be noticed from Figure 3 that PA are equably dispersed in the polymer matrix and almost embedded within PNaA-*co*-AM matrix [Fig. 3(b,c)], and no flocculation of PA particles can be observed. The fine dispersion of PA in the polymeric network facilitates the superabsorbent to form a homogeneous composition.

### Effects of initiator APS concentration on water absorbency

As shown in Figure 4, the water absorbency of the superabsorbent composite increased with increasing the concentration of APS, reaching a maximum and then decreased. Below the optimal APS concentration, the free radicals in reaction system could not be adequately formed and the polymerization and crosslinking efficiency is also lower. Thus, increasing APS concentration in this region contributes to the formation of three-dimensional hydrophilic network and the enhancement of water absorbency. However, the further increase in APS concentration may cause the shrinkage of water absorbency. According to previous report,[20] the increase of initiator concentration may decrease kinetic chain length of polymer and increase the relative amount of polymer chain ends in free-radical polymerization. Because the polymer chain ends have no contribution to the water absorbency,[21] the increase of initiator concentration certainly leads to the decrease of water absorbency.

### Effects of molar ratio of AA to AM on water absorbency

As can be seen from Figure 5, the water absorbency increased with enhancing the molar ratio of AA to AM in a feed ratio range of 0.8–1.2. As described previously,[22] the collaborative absorbent effect of —CONH, —COOH, and —$COO^-$ groups is superior to either of single —CONH, —COOH or —$COO^-$ group. Thus, the improved water-absorbing capability could be produced due to the suitable ratio of the —CONH, —COOH, and —$COO^-$ groups. However, the further increase of AA amount causes the strong hydrogen bonding interaction among polymer chains, which increased the physical crosslinking degree of the composite and decreased the water absorbency. Similar results were observed in the study of crosslinked acrylic acid and AM copolymers.[21]

### Effect of neutralization degree of AA on water absorbency

It can be noticed from Figure 6 that the water absorbency tends to increase with increasing the

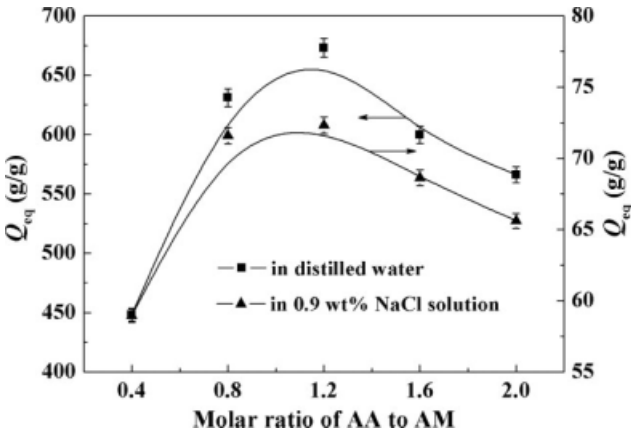


**Figure 5** Effect of molar ratio of AA to AM on water absorbency: APS concentration, 12.621 mmol/L; neutralization degree of AA, 57%; MBA concentration, 2.335 mmol/L; and PA content, 20 wt %.

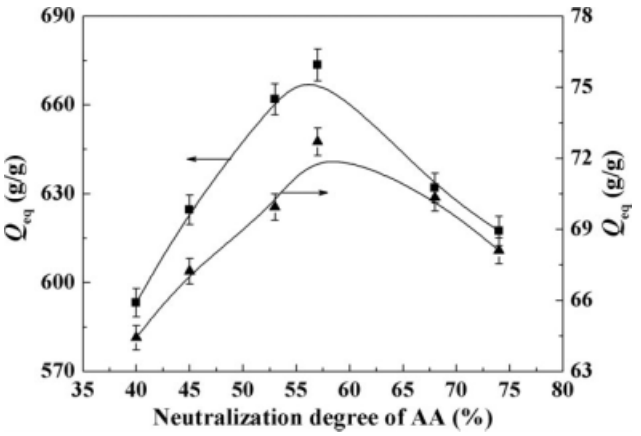


**Figure 6** Effect of neutralization degree of AA on water absorbency: APS concentration, 12.621 mmol/L; molar ratio of AA to AM, 1.2; MBA concentration, 2.335 mmol/L; and PA content, 20 wt %.

neutralization degree of AA, to reach an optimum value and then decreased. This is attributed to the facts that (i) the cooperative absorbing effect between —COOH and —$COO^-$ groups in gel network is superior to either group[22]; (ii) the neutralization of AA with NaOH solution can increase the amounts of —$COO^-$ located in gel network and enhance the osmotic pressure between gel network and swelling medium as well as rubbery elasticity among polymer chains; (iii) the decrease of amount of —COOH groups resulting from the neutralization of AA may break the hydrogen bonding network between —COOH groups, and thus the effective crosslinking density of hydrogel was reduced. However, the further increases in the neutralization degree of AA result in the introduction of more sodium ions, which reduce the electrostatic repulsion by screening the negative charges of —$COO^-$ groups and then decreased the water absorbency.

### Effects of the concentration of crosslinker MBA on water absorbency

It is well-known that properties of superabsorbent are closely related to the crosslinking degree of polymeric networks. As can be seen from Figure 7, the water absorbency of the composite abruptly decreases from 673 g/g to 262 g/g with increasing the MBA concentration from 2.34 to 11.68 mmol/L. Although crosslinker is essential to the formation of three-dimensional hydrophilic network, high crosslinker concentration may result in the generation of more crosslink points and the increase of crosslinking density. Thus, the water absorbency also correspondingly reduced. However, when the dosage of crosslinker is less, the polymeric chains cannot crosslink well and the three-dimensional hydrophilic network used for holding water fails to be effectively formed. Under this situation, the water absorbency of the superabsorbent is also low. The relationship between the equilibrium water absorbency and the MBA concentration follows the relation shown in Eq. (2).[23,24]

$$Q_{eq} = kC_{MBA}^{(-n)} \quad (2)$$

$C_{MBA}$ is the concentration of crosslinker MBA; $k$ and $n$ are constant for an individual superabsorbent, which can be obtained from the curve fitted with Eq. (2). In this series, the effect of MBA concentration on water absorbency follows the relation $Q_{eq} = 21.92C_{MBA}^{(-0.5673)}$ in distilled water and $Q_{eq} = 8.34C_{MBA}^{(-0.3546)}$ in 0.9 wt % NaCl solution.

### Effects of PA content on water absorbency

The change of PA content in composites may certainly affect their composition and water-absorbing capabilities. As shown in Figure 8, the water absorbency of the superabsorbent remarkably increased with incorporating PA, reaching an optimum absorption of 673 g/g at the PA content of 20 wt % and then decreased. The great improvement of the water absorbency can be attributed the following reasons: (i) the introduction of a lot of saline in PA enhanced the osmotic pressure difference between the internal network and the external solution, which contributes to the improvement of water absorbency; (ii) the incorporation of PA increased the roughness and surface area of superabsorbent, which is responsible for the enhancement of water absorbency (Fig. 3); and (iii) PA contains a lot of $SiO_2$, which can participate in polymerization reaction through its active —OH groups. The participation of rigid silicate in crosslinking may prevent the tangle of polymer chains and decrease the hydrogen

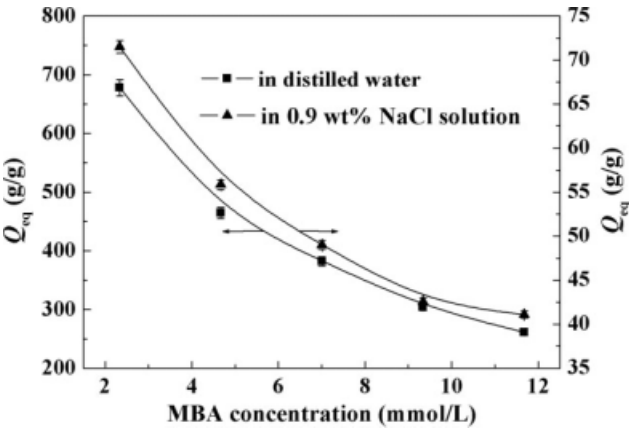


**Figure 7** Effect of MBA concentration on water absorbency: APS concentration, 12.621 mmol/L; molar ratio of AA to AM, 1.2; neutralization degree of AA, 57%; and PA content, 20 wt %.

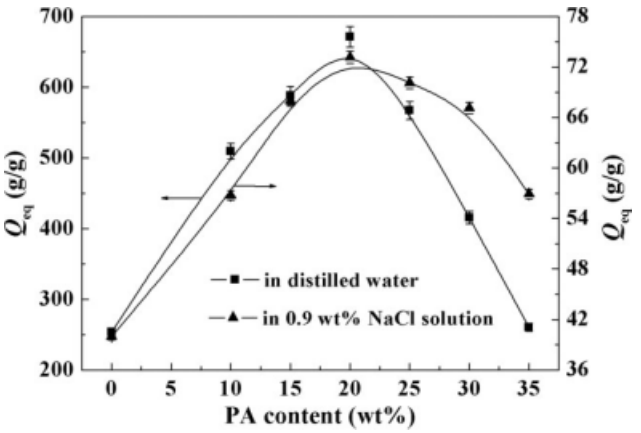


**Figure 8** Effect of PA content on water absorbency: APS concentration, 12.621 mmol/L; molar ratio of AA to AM, 1.2; neutralization degree of AA, 57%; and MBA concentration, 2.335 mmol/L.

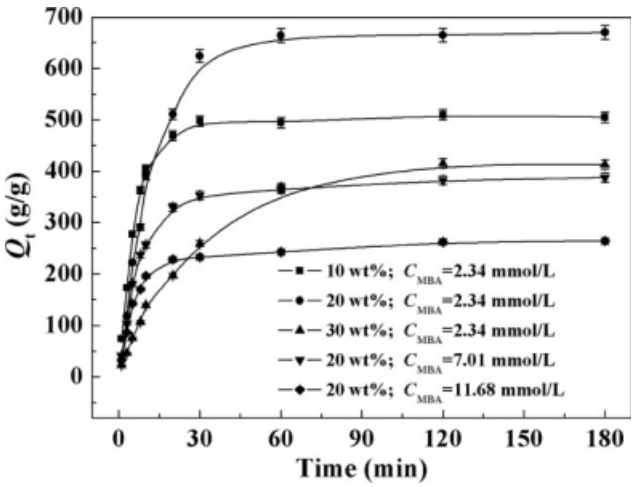


**Figure 9** Swelling kinetic curves of the superabsorbent composites with various amounts of PA and crosslinking degrees in distilled water.

bonding interaction among —$COO^-$ and —COOH groups, and then the polymeric network can be improved and the water absorbency was increased. However, the water absorbency decreased when the content of PA exceeding 20 wt %. This is because that the excessive PA powder was physically filled in the polymer network, the hydrophilicity of polymer was decreased, and the water absorbency was reduced.[25]

### Swelling kinetics

Figure 9 represented the kinetic swelling curves of the composites with certain particle sizes (180–380 μm) in distilled water. It can be observed that the swelling rate is highest at initial 10 min, and then the swelling rate is reduced and the swelling curves tend to flatter. For evaluating the kinetic swelling behaviors of the superabsorbents, the Voigt-based viscoelastic model was adopted and expressed as follows [Eq. (3)][25,26]:

$$Q_t = Q_\infty(1 - e^{-t/r}) \quad (3)$$

where $Q_t$ (g/g) is swelling capability at time $t$ (min); $Q_\infty$ (g/g) is the power parameter (g/g), denoting the theoretical equilibrium water absorbency; $r$ (min) stand for the "rate parameter," expressing the time required to reach 63% of equilibrium water absorbency. By fitting the experimental data using Eq. (3), the rate parameter $r$ and power parameter $Q_\infty$ was calculated and listed in Table I. Because the rate parameter $r$ is a measure of resistance to water permeation, a lower $r$ value may reflect a high-swelling rate.[27] According to the calculated $r$ value, it can be concluded that the swelling rate for PNa-KA-*co*-AM/PA with various amounts of PA is in the following orders: PNa-KA-*co*-AM/PA (10 wt %) > PNa-KA-*co*-AM/PA (20 wt %) > PNa-KA-*co*-AM/PA (30 wt %); for PNa-KA-*co*-AM/PA (20 wt %) with various crosslinking degrees is in the following orders: PNa-KA-*co*-AM/PA (20 wt %; $C_{MBA}$ = 11.68 mmol/L) > PNa-KA-*co*-AM/PA (20 wt %; $C_{MBA}$ = 7.01 mmol/L) > PNa-KA-*co*-AM/PA (20 wt %; $C_{MBA}$ = 2.34 mmol/L).

### Effects of saline solution on water absorbency

The external saline usually has great influence on the swelling properties of the composites when it was used as water-manageable material in practical application. As shown in Figure 10, the water absorbency of PNa-KA-*co*-AM/PA composites rapidly decreased with increasing the concentration of NaCl solution. This is because that the osmotic pressure difference between internal gel network and external solution decreased and the screening effect of counterion, e.g., $Na^+$ to negative —$COO^-$ groups enhanced with increasing the saline concentration. The driven force for water diffusing into superabsorbent network was weakened and the water absorbency decreased. The effect of the

**TABLE I**
**Swelling Kinetic Parameters of the PNa-KA-*co*-AM/PA Superabsorbent Composites with Different Content of PA and Crosslinking Degree**

| Samples | $Q_\infty$ (g/g) | $r$ (min) |
|---|---|---|
| 10 wt %; $C_{MBA}$ = 2.34 mmol/L | 502 | 6.38 |
| 20 wt %; $C_{MBA}$ = 2.34 mmol/L | 671 | 12.94 |
| 30 wt %; $C_{MBA}$ = 2.34 mmol/L | 416 | 28.63 |
| 20 wt %; $C_{MBA}$ = 7.01 mmol/L | 374 | 8.37 |
| 20 wt %; $C_{MBA}$ = 11.68 mmol/L | 250 | 6.71 |

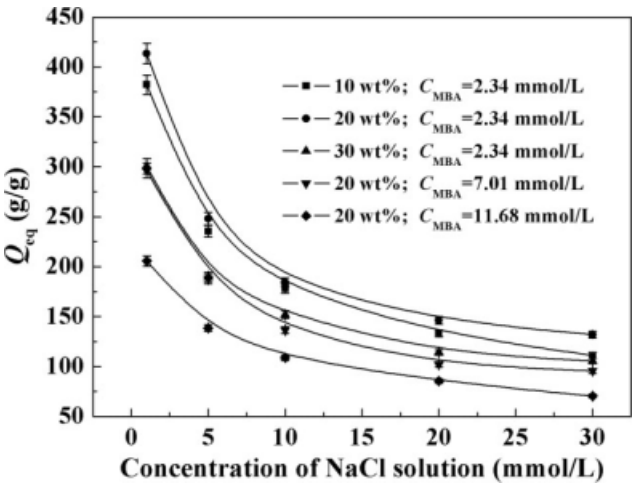


**Figure 10** Effects of saline solutions with different concentration on water absorbency.

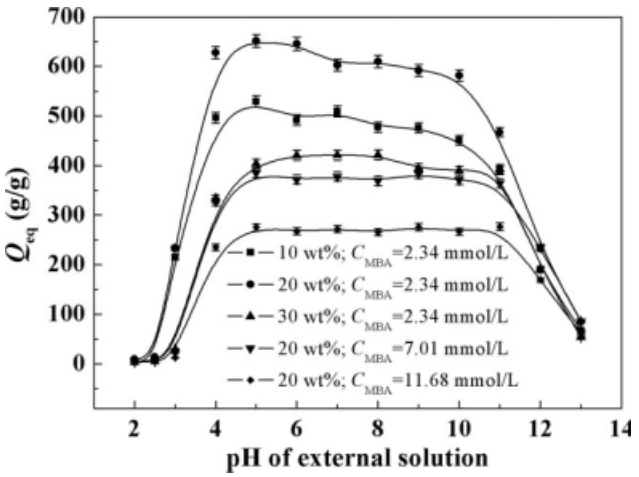


**Figure 11** Effect of pHs of external solution on the water absorbency.

concentration of NaCl solution on water absorbency follows the relationship shown in Eq. (4).[23]

$$Q_{eq} = kC_{saline}^{(-n)} \quad (4)$$

$C_{saline}$ is the concentration of saline solution; $k$ and $n$ are power law constants for an individual superabsorbent, which can be obtained from the curve fitted with Eq. (4). The calculated constants were listed in Table II. It can be seen that the exponent $n$ decreases with increasing the content of PA. In addition, the exponent $n$ of sample decreased with increasing the crosslinking degree of the superabsorbent composites. This information indicates that the incorporation of PA and the increase of crosslinking degree are favorable to improve the salt-resistant properties.

### Effect of external pHs solution on water absorbency

In practical application, the adaptability of agricultural superabsorbent to the pHs of external aqueous media or soil is also a significant factor. In this section, the equilibrium water absorbency of PNa-KA-*co*-AM/PA with various PA contents and crosslinking degrees were studied at various pHs ranged from 2 to 13 (Fig. 11). It deserves to be noticed that the superabsorbent composites can keep high water absorbency at a wide pH range from 4 to 11. This tendency can be attributed to the fact that the —$COO^-$ groups can convert to —COOH groups in acid media and the —COOH groups can convert to —$COO^-$ groups in basic environment, forming a buffer system.[15,28] The similar behavior can also be observed in previous report[29] and is very advantageous to the use of superabsorbent in various soils for agricultural and ecological projects. However, the buffer action may disappear in the case of pH $<$ 4 or pH $>$ 11. After the buffer action disappeared, the osmotic swelling pressure as well as the electrostatic repulsion among —$COO^-$ groups was decreased,[30] which ultimately reduced the equilibrium water absorbency of the superabsorbent.

**TABLE II**
**Power Law Constants for Swelling Dependency of PNa-KA-*co*-AM/PA with Different Content of PA and Crosslinking Degree on the Concentration of NaCl Solution**

| Samples | $k$ | $n$ |
|---|---|---|
| 10 wt %; $C_{MBA}$ = 2.34 mmol/L | 386 | 0.3429 |
| 20 wt %; $C_{MBA}$ = 2.34 mmol/L | 415 | 0.3400 |
| 30 wt %; $C_{MBA}$ = 2.34 mmol/L | 303 | 0.3070 |
| 20 wt %; $C_{MBA}$ = 7.01 mmol/L | 300 | 0.3339 |
| 20 wt %; $C_{MBA}$ = 11.68 mmol/L | 209 | 0.2912 |

### Potassium-release characteristics

Because PA contains plentiful potassium elements which are soluble in water, incorporation of PA into superabsorbent endow it with potassium-release characteristics. As shown in Figure 12, the potassium-release amounts of the composites in distilled water increased with prolonging the immersing time, and then tend to flat after 1 h. The composite with higher PA content can release more potassium at each given moment than that with low PA content. For the superabsorbent composites with 10, 20, and 30 wt % of PA, the total potassium-release amounts can reach 2.38, 5.43, and 8.80 mg/g, respectively.

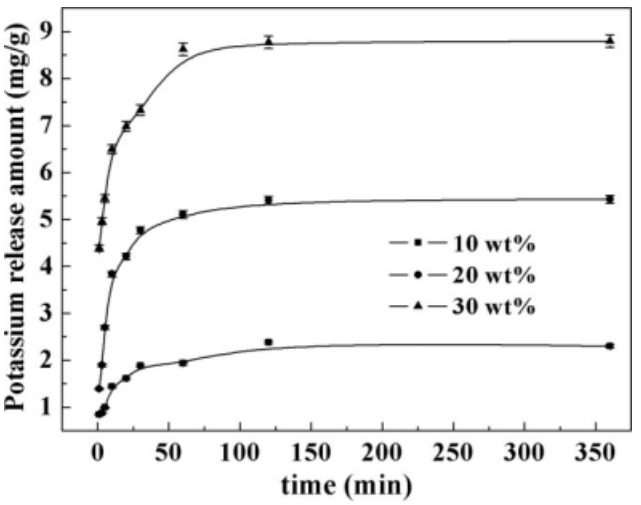


**Figure 12** Potassium-release curves of the superabsorbent composites with different content of PA in distilled water.

## CONCLUSIONS

As a part of efforts to develop a novel agricultural superabsorbent with both water-saving and fertilizer-release characteristics, the superabsorbent composite PNa-KA-*co*-AM/PA was prepared through the polymerization among NaA, AM, and PA in aqueous solution. The synthesis conditions were optimized as follows: initiator concentration, 12.621 mmol/L; molar ratio of AA to AM, 1.2; total neutralization degree of AA, 57%; crosslinker concentration, 2.335 mmol/L; and PA content, 20 wt %. The superabsorbent composite prepared under optimal conditions exhibits the best absorption of 673 g/g in distilled water and 73 g/g in 0.9 wt % NaCl solution. FTIR and SEM analysis showed that the polymerization reaction occurred and PA was uniformly dispersed in the polymeric matrix without agglomerate. The superabsorbent composites can release potassium 2.38, 5.43, and 8.80 mg/g of sample in distilled water for the composites containing 10, 20, and 30 wt % PA, respectively. The incorporation of PA into superabsorbent network not only reduce the production cost, but also enhance the thermal stability and the water-absorbing capabilities of the superabsorbent composites, and endow such material with potassium fertilizer-release characteristics.

## References

1. Chen, P.; Zhang, W. A.; Luo, W.; Fang, Y. E. J Appl Polym Sci 2004, 93, 1748.
2. Puoci, F.; Iemma, F.; Spizzirri, U. G.; Cirillo, G.; Curcio, M.; Picci, N. Am J Agric Biol Sci 2008, 3, 299.
3. Karada, E.; Saraydin, D.; Caldiran, Y.; Güven, O. Polym Adv Technol 2000, 11, 598.
4. Elias, P. K.; George, N. V. Ind Eng Chem Res 1994, 33, 1623.
5. Jarosiewicz, A.; Tomaszewska, M. J Agric Food Chem 2003, 51, 413.
6. Zhan, F. L.; Liu, M. Z.; Guo, M. Y.; Wu, L. J Appl Polym Sci 2004, 92, 3417.
7. Zheng, T.; Liang, Y. H.; Ye, S. H.; He, Z. Y. Biosys Eng 2009, 102, 44.
8. Wu, L.; Liu, M. Z. Carbohydr Polym 2008, 72, 240.
9. Chen, L.; Xie, Z. G.; Zhuang, X. L.; Chen, X. S.; Jing, X. B. Carbohydr Polym 2008, 72, 342.
10. Guo, M. Y.; Liu, M. Z.; Hu, Z.; Zhan, F. L.; Wu, L. J Appl Polym Sci 2006, 96, 2132.
11. Liang, R.; Yuan, H. B.; Xi, G. X.; Zhou, Q. X. Carbohydr Polym 2009, 77, 181.
12. Hua, S. B.; Wang, A. Q. Polym Adv Technol 2008, 19, 1009.
13. Chu, M.; Zhu, S. Q.; Li, H. M.; Huang, Z. B.; Li, S. Q. J Appl Polym Sci 2006, 102, 5137.
14. Zhang, J. P.; Li, A.; Wang, A. Q. Polym Adv Technol 2005, 16, 813.
15. Wang, W. B.; Wang, A. Q. J Appl Polym Sci 2009, 112, 2102.
16. Schrauzer, G. N. U.S. Pat. 10/625,138 (2003).
17. Li, A.; Wang, A. Q.; Chen, J. M. J Appl Polym Sci 2004, 92, 1596.
18. Taunk, K.; Behari, K. J Appl Polym Sci 2000, 77, 39.
19. Qi, X. H.; Liu, M. Z.; Chen, Z. B.; Zhang, F., Zhao, L. Polym Adv Technol, submitted; Doi: 10.1002/pat.1416.
20. Allcock, H. R.; Frederick, W. L. Contemporary Polymer Chemistry; Prentice-Hall: Englewood Cliffs, NJ, 1981.
21. Liu, Z. S.; Remple, G. L. J Appl Polym Sci 1997, 64, 1345.
22. Wu, J. H.; Lin, J. M.; Li, G. Q.; Wei, C. R. Polym Int 2001, 50, 1050.
23. Flory, P. J. Principles of Polymer Chemistry; Cornell University Press: New York, 1953.
24. Kabiri, K.; Omidian, H.; Hashemi, S. A.; Zohuriaan-Mehr, M. J. Eur Polym J 2003, 39, 1341.
25. Lin, J. M.; Wu, J. H.; Yang, Z. F.; Pu, M. L. Macromol Rapid Commun 2001, 22, 422.
26. Omidian, H.; Hashemi, S. A.; Sammes, P. G.; Meldrum, I. G. Polymer 1998, 39, 6697.
27. Pourjavadi, A.; Mahdavinia, G. R. Turk J Chem 2006, 30, 595.
28. Lee, W. F.; Wu, R. J. J Appl Polym Sci 1996, 62, 1099.
29. Liu, J. H.; Wang, A. Q. J Appl Polym Sci 2008, 110, 678.
30. Kiatkamjornwong, S.; Chomsaksakul, W.; Sonsuk, M. Radiat Phys Chem 2000, 59, 413.